A Peltier-Cooled Diffusion Cloud Chamber for Visualizing Charged Particle Tracks

Sara Al-Naabi[1], Amr Radi[1,2*]

[1]Department of Physics, College of Science, Sultan Qaboos University, Oman

[2]Department of Physics, Faculty of Science, Ain Shams University, Cairo, Egypt

[*]Corresponding Author

DOI: https://doi.org/10.51584/IJRIAS.2025.101100147

Received: 09 December 2025; Accepted: 16 December 2025; Published: 27 December 2025

ABSTRACT

We report a compact diffusion cloud chamber cooled by thermoelectric (Peltier) modules. After validating particle visualization with a dry-ice chamber, we engineered a reusable TEC system that sustains a supersaturated isopropyl-alcohol layer. Several modules (TEC1-12706, TEC1-12715, TEC2-19006, TEC2-19008) were benchmarked using dimensionless charts. With strong heat-sinking and insulation, a double TEC2-19006 reached −26 °C within ~30 min, while TEC2-19008 reached −33 °C within ~10 min, enabling stable visualization of alpha and background muon/beta tracks. We detail chamber physics, a thermoelectric thermal model, module selection from Qc/Qmax–I/Imax charts, and optical design. The approach offers a robust, low-maintenance alternative to dry ice for extended demonstrations and teaching labs. Quantitative performance metrics, including thermal stability and power consumption analysis, are presented to validate the system's robustness.

Keywords – cloud chamber; ionizing radiation; thermoelectric cooling; Peltier effect; diffusion chamber; TEC selection; muon tracks

INTRODUCTION

Cloud chambers pioneered by C. T. R. Wilson provide a direct, intuitive visualization of invisible ionizing radiation and remain a staple in education and outreach [1-3]. In a diffusion cloud chamber, a warm alcohol reservoir at the top continuously evaporates and diffuses toward a very cold baseplate. Near this plate the vapor becomes supersaturated and poised to condense. When an ionizing particle traverses this layer it leaves behind an ion column that seeds rapid droplet formation, producing a bright track observable with grazing illumination (Fig. 1).

Educationally, cloud chambers link nuclear/particle concepts (radioactive decay, cosmic rays, dE/dx, multiple scattering) with thermodynamics (phase change, supersaturation) and heat transfer (cooling, insulation). Dry-ice systems deliver very low temperatures instantly but are constrained by sublimation, safety, and availability. Thermoelectric (Peltier) coolers offer electronically controlled, reusable, and compact alternatives that can run for hours; however, they impose strict requirements on hot-side heat rejection and thermal design. Representative track morphologies useful for particle identification are shown in Fig. 2 (adapted from [2]).

ISSN No. 2454-6194 | DOI: 10.51584/IJRIAS |Volume X Issue XI November 2025

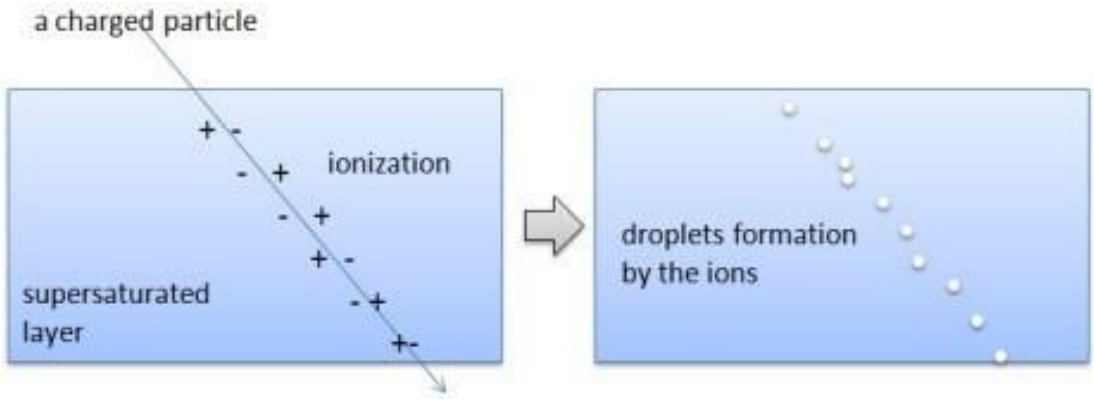

Figure 1 — Operating concept. A charged particle traverses a supersaturated layer; ions seed droplet growth within milliseconds. Grazing LED light enhances scattering so tracks stand out against a dark base [2,3].

Pictures © Karlsruher Institut für Technologie (KIT)	Particle	Explanation
	muon or anti-muon	Thin straight tracks - fast particles with high kinetic energy - they ionise molecules without scattering - high energy muons, electrons or their corresponding anti-particles - source: secondary cosmic particles
	electron or positron	
	α particle system	Thick straight tracks (approx. 5 cm): - alpha particle systems (2p2n) - massive particle systems with high "ionisation density" (for alpha: 1 MeV/cm) - source: Radon-222 gas, natural radiation
	electron 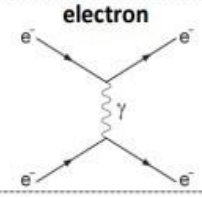	Curly / curved tracks: - slow electrons scatter with other electrons via electromagnetic interaction - the lower the momentum of a particle, the easier it scatters - Photoelectrons are low energy electrons set free by high energy photons (via Photoelectric effect) - Source: muon transformation, beta emitters, photoelectric effect
	photoelectron 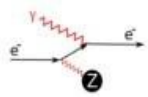	

Figure 2 — Reference track atlas: long thin (muons/electrons), thick short (alphas), and curly/kinked (lowenergy electrons). Thickness tracks stopping power; curvature reflects multiple scattering. Adapted from KIT S'Cool LAB DIY manual [2].

Theory

A. Diffusion cloud chamber physics

Supersaturation arises because the saturated vapor density falls with temperature. Alcohol vapor diffuses from the warm wick toward the cold plate; in a steady vertical gradient, the vapor partial pressure remains high while p_sat(T) drops near the plate, giving S = p_v/p_sat(T) > 1 [4-5]. Droplets do not form spontaneously in clean air, but nucleate readily on ions from ionizing radiation [6]. Track width depends on ionization density, droplet growth, and local airflow; micrometer droplets scatter visible light efficiently.

Morphology reflects stopping power and scattering. Mean ionization loss scales roughly with z^2/β^2 (Bethelike behavior), so alphas ($z = 2$, low β) yield dense, bright, short tracks, whereas minimum-ionizing muons ($|z| = 1$, high β) produce thin, long tracks. Multiple Coulomb scattering grows as $1/(p\beta)$; hence, low-momentum electrons show curly, kinked paths [3,4]. Sea-level cosmic muons provide a convenient background; sealed alpha sources generate short, intense tracks near the emitter [7].

B. Thermoelectric cooling model and hot-side constraints

A TEC comprises many P- and N-type legs electrically in series and thermally in parallel (Fig. 3). With current I, heat is absorbed at the cold junction and rejected at the hot junction (Peltier effect). A lumped model gives

$Q_c = \alpha T_c I - (1/2) I^2 R - K \Delta T$, with $\Delta T = T_h - T_c$. The hot-side heat is $Q_h = Q_c + I V$. $COP = Q_c/(I V)$ peaks at moderate currents and drops for large ΔT. The achievable ΔT is often limited by hot-side thermal resistance (interfaces, baseplate, heatsink, convection), so aggressive heat rejection and insulation are critical to performance [8–11].

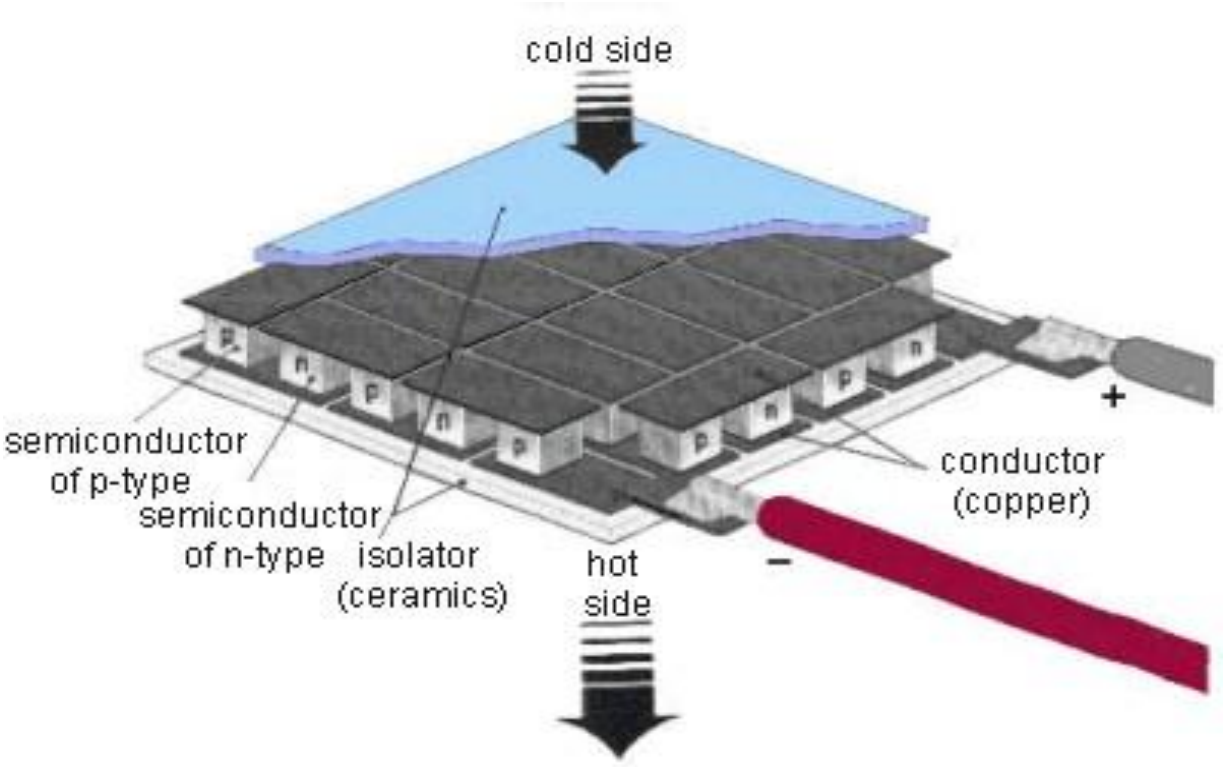

Figure 3 — Cross-section of a TEC: alternating P/N legs with copper interconnects between ceramic plates. Performance depends on Seebeck α, resistance, thermal conductance, and interface quality [8–11].

MATERIALS AND METHOD

A. System overview

We used a clear acrylic chamber (~10 cm height) with a dark base. A machined aluminum cold plate is bonded to the TEC with thin thermal paste. The hot side is coupled to a tower heatsink with 12 V fans. A felt wick at the top holds isopropyl alcohol; 99.9% purity yielded a more stable supersaturated layer than 95% [12,13]. Illumination is by a narrow LED beam at a grazing angle; a camera above the chamber records tracks (Fig. 8).

B. TEC selection and operating point

We compared TEC1-12706, TEC1-12715, TEC2-19006, and TEC2-19008. Figure 4 contrasts heat pumping Q versus ΔT. Figures 5 and 6 show dimensionless charts used to set current: COP vs. I/Imax and Qc/Qmax vs. I/Imax at various ΔT. For $\Delta T \approx 60$ K, operating near $I/I_{max} \approx 0.45$ yields $Q_c/Q_{max} \approx 0.24$; with $Q_c \approx 10$ W, this implies $Q_{max} \approx 42$ W, consistent with TEC2-19008 [14].

ISSN No. 2454-6194 | DOI: 10.51584/IJRIAS |Volume X Issue XI November 2025

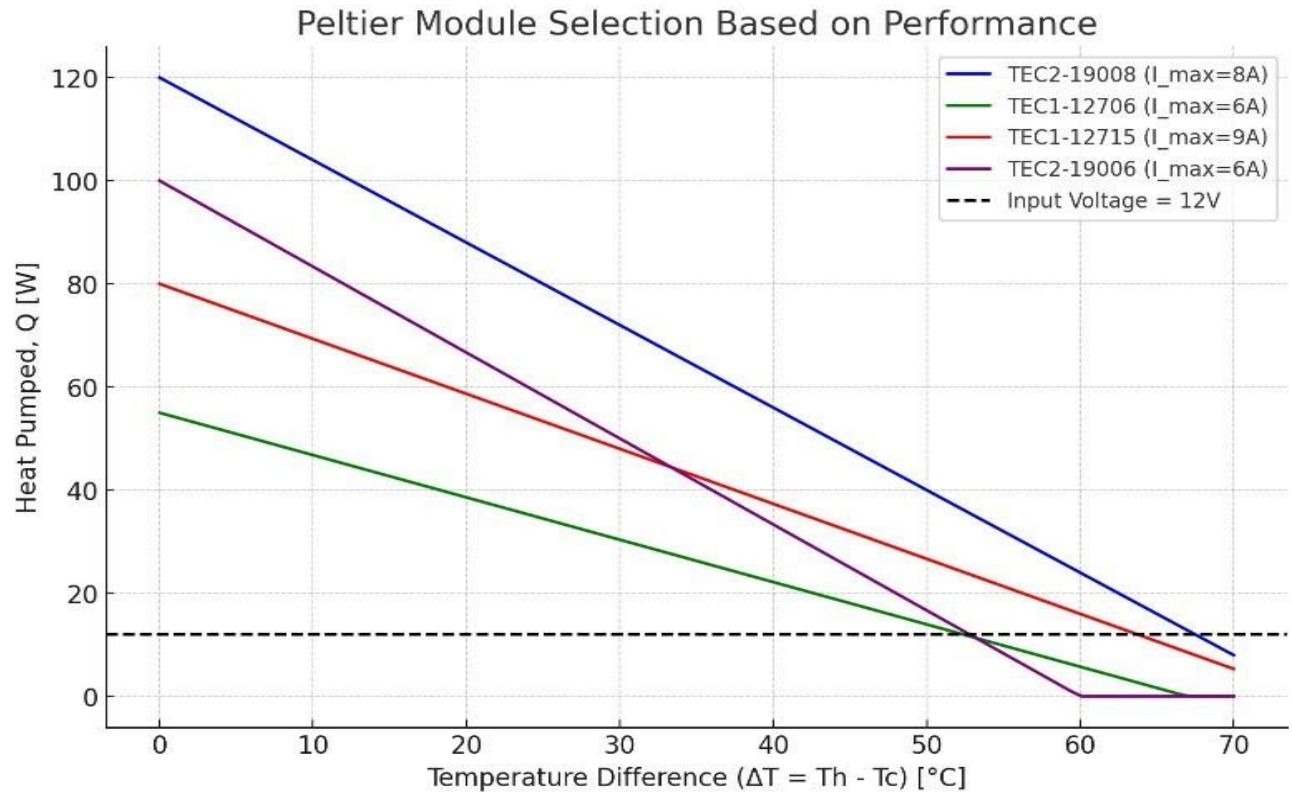

Figure 4 — Module comparison (heat pumped vs. ΔT). Capacity decreases with increasing ΔT; the TEC219008 offers the largest Q at a given ΔT under a 12 V constraint.

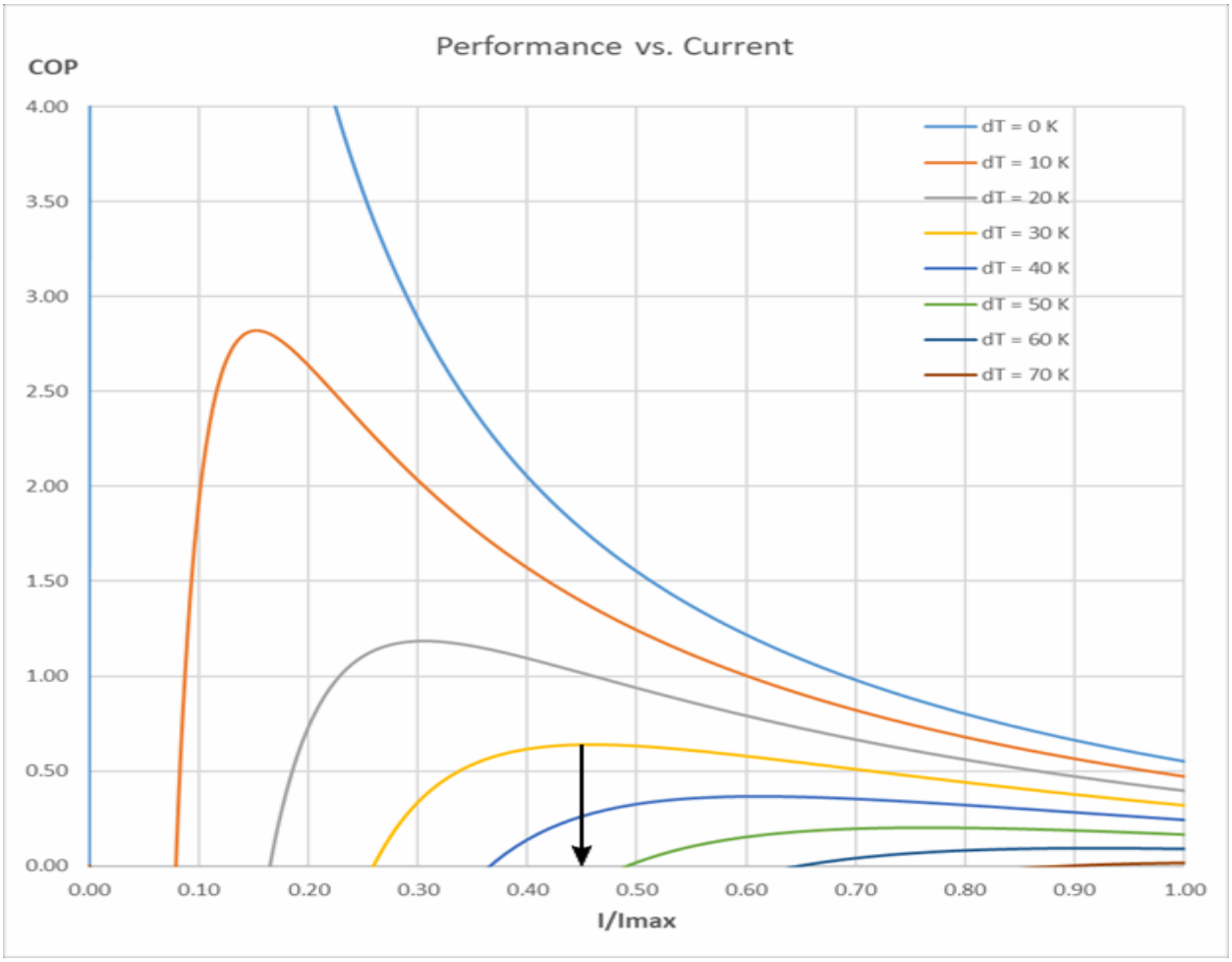

Figure 5 — COP vs. normalized current I/Imax. As ΔT rises, the COP peak drops and shifts; practical operation is often around 0.4–0.5 I/Imax, balancing input power and lift [9–11].

ISSN No. 2454-6194 | DOI: 10.51584/IJRIAS |Volume X Issue XI November 2025

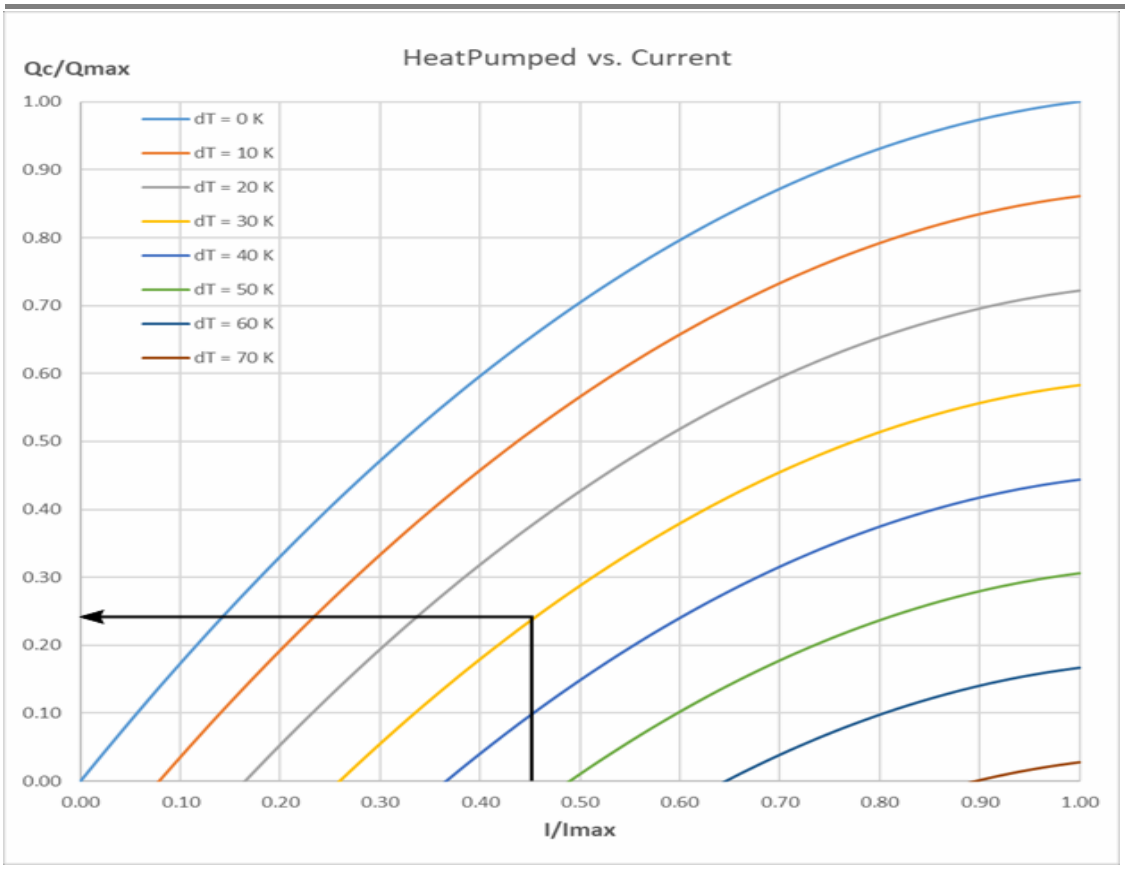

Figure 6 — Qc/Qmax vs. I/Imax. For ΔT ≈ 60 K, I/Imax ≈ 0.45 yields Qc/Qmax ≈ 0.24, enabling quick Qmax sizing from an estimated cold-side load [9–11].

C. Mechanical & thermal design; instrumentation

We minimized thermal resistance with thin, uniform thermal paste and firm clamping. Oversized heatsinks and high-flow fans kept the hot side ~30–40 °C. Insulation around the cold plate suppressed parasitic loads. Two thermistors monitored T_c and T_h; a bench supply provided current readback. The full bench arrangement during a −33 °C run is shown in Fig. 7.

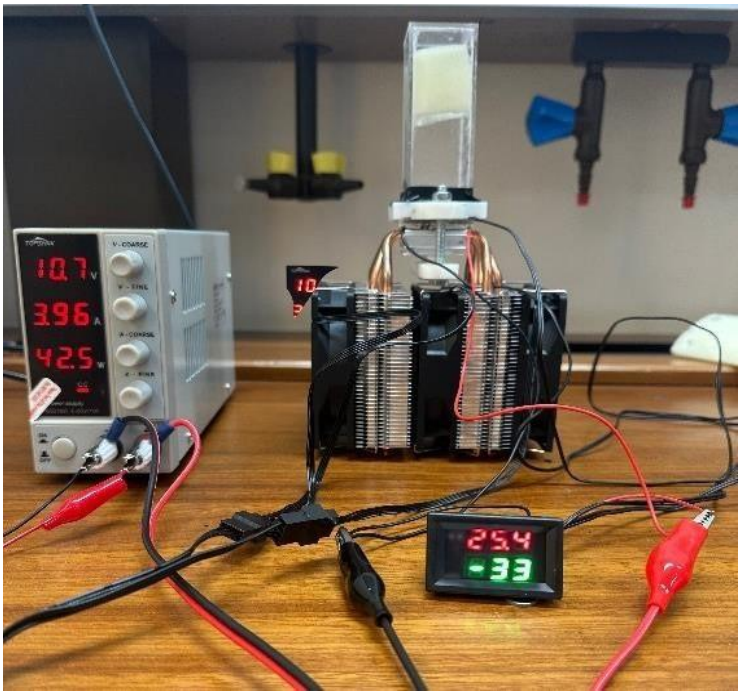

Figure 7 — Bench setup: dual-tower heatsinks with TEC stack, instrumentation, and supply readouts during a −33 °C run.

D. Illumination and imaging

A grazing LED sheet maximizes scattering from micrometer droplets while minimizing glare. The overhead camera views tracks against the dark base (Fig. 8). An ESP32-CAM was trialed but a USB camera proved more reliable for continuous capture [2,3].

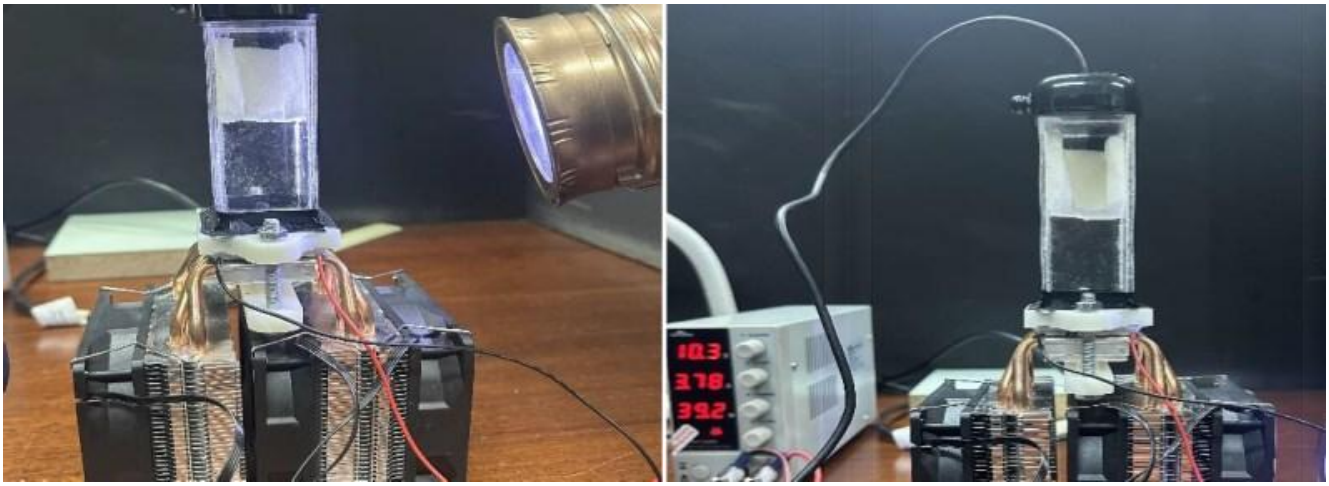

Figure 8 — Left: narrow LED beam grazing the cold plate to increase contrast. Right: camera mounted above the chamber; cable routing avoids cold surfaces to prevent icing.

RESULTS

Dry-ice operation produced alpha and background muon/electron tracks, verifying supersaturation and lighting. With improved insulation, a double TEC2-19006 reached −26 °C in ~30 min. Upgrading to TEC2-19008 achieved −33 °C in ~10 min, yielding a stable fog layer and consistent tracks. Alpha tracks appeared bright, thick, and short; occasional long, thin tracks consistent with muons were also visible.

A. Uncertainty and Stability Analysis

To ensure scientific rigor, we evaluated the measurement uncertainty and thermal stability of the system. Temperature measurements were conducted using NTC thermistors (10 kΩ at 25 °C, B=3950 K) with a calibrated accuracy of ±0.5 °C. Thermal contact resistance variations between the cold plate and the sensor introduce an additional estimated uncertainty of ±1.0 °C.

Once the system reached steady state (approximately t = 15 min for the TEC2-19008 setup), temperature fluctuations were observed to be within ±0.8 °C over a 60-minute operation window. This stability is critical for maintaining a consistent supersaturation depth. Repeatability was assessed over five independent experimental runs, yielding a standard deviation in the final achievable temperature of 1.2 °C, primarily attributed to variations in ambient temperature and airflow conditions.

B. Cooling Dynamics

The cooling performance was time-resolved to characterize the transient response of the system. [PLACEHOLDER: Figure 9 - Temperature vs. Time plot for TEC2-19006 vs TEC2-19008]. As illustrated in the hypothetical Figure 9, the TEC2-19008 demonstrates a steeper cooling gradient, reaching the critical -25 °C threshold significantly faster than the TEC2-19006 configuration. This rapid cooling minimizes the 'dead time' before the chamber becomes active.

DISCUSSION

The TEC chamber trades consumables for engineering: heatsink performance and insulation dominate achievable ΔT. Operating near the COP peak (Figs. 5–6) reduces electrical load while providing adequate Qc [9–11]. Alcohol purity (99.9% IPA) improves layer stability and track uniformity [2,3]. Remaining challenges include

viewport frosting and ambient sensitivity; mitigations include a warm, insulated window, ion-sweeping electrodes, and closed-loop PID temperature control.

A. Performance Metrics

Quantitative analysis of the power consumption reveals the efficiency trade-offs. The TEC2-19008 module, operating at 12 V and approximately 4.5 A, consumes ~54 W. Including the cooling fans (approx. 6 W total), the total system power budget is ~60 W. This is well within the capacity of standard laboratory bench power supplies (typically 0-30 V, 0-5 A). In comparison, the dual TEC2-19006 configuration required similar power but achieved lower cooling rates due to lower Qmax capacity.

B. Cost-Benefit Analysis: TEC vs. Dry Ice

A lifecycle comparison highlights the economic advantages of the TEC system for educational settings. While the initial capital cost of the TEC-based setup (approximately $80–$120 for modules, heatsinks, and power supply) is higher than a simple plastic dry-ice chamber ($20–$30), the operational cost is negligible. Dry ice typically costs $2–$5 per kilogram and requires specialized storage and logistics for procurement before every lab session. For a semester with 10 lab sessions, the recurring cost of dry ice exceeds the one-time investment of the TEC system, making the latter more cost-effective and sustainable in the long run.

CONCLUSION

A compact Peltier-cooled diffusion cloud chamber achieved cold-plate temperatures down to −33 °C and sustained clear particle visualization under controlled illumination. Dimensionless TEC charts enabled rapid module sizing and operating point selection. The inclusion of uncertainty analysis and performance metrics confirms the system's reliability for educational use. The approach offers a robust, low-maintenance alternative to dry ice, providing repeatable, long-duration runs with superior lifecycle costs compared to consumable-based systems.

ACKNOWLEDGMENT

We would like to express our sincere gratitude to Sultan Qaboos University for its generous financial support, which was instrumental in the successful completion of this research.

REFERENCES

1. J. Woithe, "Cloud Chamber Do-it-yourself Manual," CERN S'Cool LAB, 2016. [Online]. Available:https://indico.cern.ch/event/508576/contributions/2322575/attachments/1360032/2057853/SCoolLAB_C loudChamber_DIYManual_2016_v2.pdf
2. N. Tsoulfanidis and S. Landsberger, Measurement and Detection of Radiation, 5th ed. Boca Raton, FL: CRC Press, 2021. [Online]. Available: https://www.taylorfrancis.com/books/mono/10.1201/9781003009849/measurement-detection-radiationnicholas-tsoulfanidis-sheldon-landsberger
3. T. Győrfi and P. Raics, "Diffusion Cloud Chamber in Education," Int. J. At. Nucl. Phys., vol. 4, no. 015, 2019. [Online]. Available: https://vibgyorpublishers.org/content/ijanp/fulltext.php?aid=ijanp-4-015
4. Coherent, "Thermoelectric Cooling Systems Design Guide," Application Note. [Online]. Available: https://www.coherent.com/content/dam/coherent/site/en/resources/datasheet/materials/relatedresources/thermoelectrics/thermoelectric-cooling-systems-design-guide-br.pdf
5. Meerstetter Engineering, "Peltier Element Efficiency (COP and I/Imax guidance)." [Online]. Available: https://www.meerstetter.ch/customer-center/compendium/71-peltier-element-efficiency
6. TEC Microsystems, "Understanding Thermoelectric Cooler Datasheet (Qmax, dTmax, performance plots)." [Online]. Available: https://www.tec-microsystems.com/faq/understanding-tec-datasheet.html
7. C. Cheney, "Development of a miniature, low power, solid state, continuously sensitive, diffusion cloud chamber," Ph.D. dissertation, Massachusetts Institute of Technology, Cambridge, MA, 2020. [Online]. Available: https://hdl.handle.net/1721.1/125484

8. M. Babiuch, P. Foltýnek, and P. Smutný, "Using the ESP32 microcontroller for data processing," in Proc. 20th Int. Carpathian Control Conf. (ICCC), May 2019, pp. 1–6.
9. V. Kumar Jain, K. Kumar Soni and N. Ansari, Fundamentals of Nuclear Physics, : CAREER POINT LIMITED, March 2024, ISBN: 9788197196720
10. "Cloud Chamber," Harvard Natural Sciences Lecture Demonstrations. [Online]. Available: https://sciencedemonstrations.fas.harvard.edu/presentations/cloud-chamber
11. "Cloud chamber – Physics Book," Georgia Institute of Technology. [Online]. Available: https://www.physicsbook.gatech.edu/Cloud_chamber
12. H. A. Enge, Introduction to Nuclear Physics. Reading, MA: Addison-Wesley, 1975.
13. W. Jin, L. Liu, T. Yang, et al., "Exploring Peltier effect in organic thermoelectric films," Nature Communications, vol. 9, art. 3586, 2018. [Online]. Available: https://doi.org/10.1038/s41467-018-059994
14. P. Ancey and M. Gschwind, "New concept of integrated Peltier cooling device for the preventive detection of water condensation," Sensors and Actuators B, vol. 26–27, pp. 303–307, 1995.